arXiv:1407.4180v1 [astro-ph.SR] 16 Jul 2014

Slipping Magnetic Reconnection Triggering a Solar Eruption of a Triangle-flag Flux Rope

Ting Li & Jun Zhang

ABSTRACT

We firstly report the simultaneous activities of a slipping motion of flare loops and a slipping eruption of a flux rope in 131 Å and 94 Å channels on 2014 February 02. The east hook-like flare ribbon propagated slippingly at a speed of about 50 km s^{-1}, which lasted about 40 min and extended by more than 100 Mm, but the west flare ribbon moved in the opposite direction with a speed of 30 km s^{-1}. At the later phase of the flare activity, a "bi-fan" system of flare loops was well developed. The east footpoints of the flux rope showed an apparent slipping motion along the hook of the ribbon, simultaneously the fine structures of the flux rope rose up rapidly at a speed of 130 km s^{-1}, much faster the whole flux rope. We infer that the east footpoints of the flux rope are successively heated by a slipping magnetic reconnection during the flare, which results in the apparent slippage of the flux rope. The slipping motion delineates a "triangle-flag surface" of the flux rope, implying that the topology of a flux rope is more complex than anticipated.

Subject headings: Sun: magnetic reconnection — Sun: flares — Sun: filaments, prominences

1. Introduction

Magnetic reconnection causes the transition from magnetic energy to kinetic energy of accelerated particles and thermal energy. Energetic particles propagating along the reconnected magnetic fields can impact the chromosphere, which results in the formation of flare ribbons (Schmieder et al. 1996; Asai et al. 2004). Flare ribbons are the footpoints of flare loops, which are formed due to chromospheric evaporation (Milligan & Dennis 2009; Ning et al. 2009). In the classical two-dimensional (2D) magnetic reconnection model called the

Key Laboratory of Solar Activity, National Astronomical Observatories, Chinese Academy of Sciences, Beijing 100012, China; [liting;zjun]@nao.cas.cn

CSHKP model (Carmichael 1964; Hirayama 1974), the magnetic field lines stretched by the erupting flux rope successively reconnect at places where the magnetic connectivity is discontinuous. A pair of flare ribbons are located in opposite magnetic polarities and parallel to the magnetic polarity inversion line (PIL).

However, magnetic reconnection can also take place at sites where the magnetic connectivity is continuous but with a strong gradient, i.e., quasi-separatrix layers (QSLs; Priest & Démoulin 1995; Démoulin et al. 1996). The flare ribbons are found to be along or just near the intersection of QSLs, implying that reconnection can occur in the absence of discontinuity (Démoulin et al. 1997; Guo et al. 2013). Three-dimensional (3D) magnetohydrodynamic (MHD) simulations showed that magnetic field lines passing through QSLs can successively reconnect and exchange their connectivity with neighboring field lines, which resulted in the apparent slipping motion (Pontin et al. 2005; De Moortel & Galsgaard 2006; Aulanier et al. 2006).

Up to now, direct observations of slipping magnetic reconnection are very rare. Aulanier et al. (2007) firstly reported fast bidirectional motions of coronal loops, supportive of the existence of slipping magnetic reconnection. Recently, Dudík et al. (2014) presented the detailed observations that the flare loops exhibited apparent slipping motion during an eruptive X1.4 flare. In this work, the slipping motion of flare loops and the eruption of a "triangle-flag" flux rope are simultaneously observed by the *Solar Dynamics Observatory* (*SDO*; Pesnell et al. 2012). Here, we focus on the evolution processes of the flare ribbons, the slipping flare loops and the erupting flux rope.

2. Observations and Data Analysis

On 2014 February 02, a C8.9 flare occurred in NOAA AR 11967, including two negative-polarity flare ribbons (NR1 and NR2 in Figure 1) and one positive-polarity ribbon (PR in Figure 1). The flare loops connecting the hook-like NR1 and the PR exhibited an apparent slipping motion with the west and east ends moving in opposite directions. The slipping motion of the east footpoints of the flux rope was also observed along the hook-like NR1.

The Atmospheric Imaging Assembly (AIA; Lemen et al. 2012) onboard the *SDO* takes full-disk images in 10 (E)UV channels at $1''.5$ resolution and high cadence of 12 s. The flux ropes and slipping flare loops could only be clearly observed in two higher-temperature EUV channels of 131 Å and 94 Å. The 131 Å channel best shows the flux rope and we focus on this channel in this study. The high-cadence 304 Å observations are used to analyze the evolution of flare ribbons. Moreover, the observations of 1600 Å and 171 Å are also used to

show the multi-wavelength appearance of this event. The 131 Å channel corresponds to a high temperature of about 11 MK (Fe VIII, Fe XXI) and the channel of 304 Å (He II) is at 0.05 MK (O'Dwyer et al. 2010; Boerner et al. 2012; Parenti et al. 2012). We also use the full-disk line-of-sight magnetic field data from the Helioseismic and Magnetic Imager (HMI; Scherrer et al. 2012) onboard *SDO*, with a cadence of ~ 45 s and a sampling of $0''.5$ pixel^{-1}.

3. Results

3.1. Evolution of Flare Ribbons and Slipping Motion of Flare Loops

Before the flare started, the partial eruption of a filament was initiated. Starting from 05:40 UT, the filament was initially disturbed and associated with EUV brightening. Then partial filament material rose up and seemed to be disconnected from its north end (Figure 1(a); see Animation 304). At about 06:20 UT, the thread-like structures overlying the filament gradually became clear and the first flux rope (FR1 in Figures 2(a) and 3) appeared. When the flare was initiated, another flux rope (FR2) gradually appeared at 07:14 UT (Figure 2(a)). The appearance of the FR2 was associated with the partial activation of the filament, and the activated filament material was embedded in the structures of the FR2. The AR 11967 where the flare occurred was complex and mainly consisted of two couples of sunspots (Figure 2(b)).

Seen from AIA 304 Å images, two flare ribbons started to appear at two sides of the filament from about 07:05 UT (Figure 1(b)). The GOES soft X-ray 1−8 Å flux showed that the C8.9 flare initiated at 07:17 UT, reached its peak at 07:44 UT and ended at 07:58 UT (Figure 4(a)). The PR moved to the south and its trajectory was approximately parallel to the neutral line (Figures 1(b)-(h)). Meanwhile, the NR1 propagated in the opposite direction and delineated a hook-like morphology with a length of about 100 Mm. Afterwards, the filament was disturbed again about 1.5 hr after its activation at 05:40 UT. At about 07:10 UT, partial filament material was activated and seemed to be disconnected from its north end. The activated material moved along the strands of the filament and erupted at last (see Animation 304). Subsequently another flare ribbon (NR2 in Figures 1(c)-(h)) appeared at 07:18 UT. The HMI line-of-sight magnetograms show that the PR is located in positive-polarity fields nearby a sunspot of the AR (Figure 1(h)). Before the appearance of the PR, the north magnetic structures of the PR emerged and moved southward along the PR. The hook-like NR1 and NR2 lie at the negative-polarity region that corresponds to the faculae of the AR (Figures 1(f) and (h)). In order to analyze the propagation of the NR1 and PR, we obtain the stack plots (Figures 4(b)−(c)) along slices "A−B" and "C−D" (blue dotted lines in Figure 1(b)) in 304 Å images. The NR1 lasts about 40 min and the average velocity of

the NR1 is approximately 50 km s^{-1}. The PR has a length of about 40 Mm, and propagates to the south with a velocity of 30 km s^{-1}.

In the AIA 131 Å and 94 Å observations, the newly-formed flare loops "L1" and "L2" connecting the NR1 and PR were observed at about 07:19 UT (Figure 2(c)), when the flare started. "L1" and "L2" seemed to be crossed each other. Then flare loops "L3," "L4" and "L5" successively appeared and these flare loops formed a "bi-fan" loop system (Figure 2(f)). The apparent slipping motion of flare loops was clearly observed (Figures 2(c)-(f); Animation 131-loops). The west ends of the loops slipped to the southeast, which developed into the PR. However, the east ends moved to the north along the hook-like NR1. These slipping loops could not be observed in low-temperature channels such as 171 Å (Figure 1(g)).

3.2. Slipping Eruption of the FR1

The C8.9 flare seemed to trigger the slipping eruption of the FR1. Since the appearance of the FR1, it started to expand and rise up slowly at approximately 07:00 UT (Figures 3(a)-(b)). The east footpoints of the FR1 showed an apparent slipping motion along the hook of the NR1 (Figures 3(b)-(f); Animation 131-fluxropes). The slipping motion of the FR1 lasted about 40 min, from about 07:06 UT to 07:50 UT. Meanwhile, the formerly invisible fine structures of the FR1 became visible in succession (solid curves in Figures 3(b)-(f)). These successively visible fine structures delineated a "triangle-flag" topology of the FR1 (Figure 3(f)). However, the west footpoints of the FR1 remained at the initial position. In order to analyze the kinematic evolution of the FR1 in detail, we obtain the stack plots (Figures 4(d)−(e)) along slices "E−F" and "G−H" (Figure 3(a)). The initial rise velocity of the fine structures of the FR1 is about 20 km s^{-1} (Figure 4(d)). At about 07:24 UT, the fine structures rose upward rapidly with a velocity of 130 km s^{-1}. However, the whole FR1 rose up very slowly at a speed of 5 km s^{-1} from 07:18 UT to 07:38 UT (Figure 4(e)). Afterwards, it was deflected towards the northeast and the west end of the FR1 was broken away from the solar photosphere due to its interaction with the north bundles of loops in the north AR (Animation 131-fluxropes).

4. Summary and Discussion

We firstly report the simultaneous observations of the slipping flare loops and the erupting FR1 by SDO/AIA on 2014 February 02 in AR 11967. The "triangle-flag surface" and the fine structures, both along the erupting FR1, are also unprecedented as compared to

previous studies. The flare loops exhibited an apparent slipping motion as seen in 131 Å and 94 Å channels. The west and east footpoints of flare loops slipped in opposite directions, resulting in the "bi-fan" topology of flare loops. The east hook-like flare ribbon at the faculae of the AR propagated at a speed of about 50 km s^{-1} and extended by more than 100 Mm. The west flare ribbon moved in the opposite direction with a speed of 30 km s^{-1}, slightly smaller than the hook ribbon. Accompanying the propagation of the hook-like ribbon, the east footpoints of the FR1 showed an apparent slipping motion along the hook of the ribbon. The slipping footpoints were located nearby the position where the hook-like ribbon propagated. The fine structures of the FR1 rose upward rapidly at a speed of about 130 km s^{-1}, much faster than the whole FR1 (5 km s^{-1}). However, the west footpoints of the FR1 were compact and stationary, anchoring in positive-polarity magnetic flux concentration.

We considered the observed features of FR1 and FR2 as flux ropes for two reasons. Firstly, the intertwined and twisted structures are observed for FR1 and FR2. Gibson et al. (2004) defined a flux rope as a set of EUV loops that collectively wind around a central axial line. Secondly, FR1 and FR2 could only be observed in high-temperature channels of AIA, such as 131 Å and 94 Å. In recent literatures (e.g., Cheng et al. 2011), they are considered as high-temperature flux ropes. If FR1 and FR2 are other features (e.g., potential loops), they usually could be observed in both high- and low-temperature channels, including 171 Å, 193 Å and 131 Å and 94 Å. Thus, we are prone to name FR1 and FR2 as flux ropes rather than other features.

The magnetic fields in QSLs are continuous and hence the change in footpoint connectivity of the fields occurs at finite speed (Aulanier et al. 2007). The speed of the slipping motion is the exchange rate of connectivity of magnetic fields. According to the speed of slipping motion, Aulanier et al. (2006) gave two definitions of slip-running and slipping reconnection regimes that respectively correspond to super- and sub-Alfvénic field line fast slippage. In our observations, the slipping speeds were 30 and 50 km s^{-1}. They are comparable to the slipping speeds of coronal loops in Aulanier et al. (2007) and flare loops in Dudík et al. (2014). These speeds are sub-Alfvénic speeds, and satisfy the slipping reconnection regime.

Our observations of an eruptive flare have revealed several typical 3D physical process, including: the hook-like flare ribbon and the slippage of post-flare loops with two ends along opposite directions. However, the CSHKP model could not completely account for these observed properties. In the classical CSHKP model, the flare ribbons are almost parallel to the PIL and flare loops have similar shapes that are approximately perpendicular to the PIL. Recently, 3D extensions to the CSHKP model have been carried out by Aulanier et al. (2012) and Janvier et al. (2013). They have simulated the 3D MHD evolution process of a torus-

unstable erupting flux rope during an eruptive flare, and the slipping-running reconnection of field lines is well reproduced in their simulations. Magnetic field lines undergo successive reconnections as they cross the QSLs and the continuous rearrangements of field lines along the QSLs generate the apparent slipping motion of field line footpoints. Their "standard solar flare model in 3D" matches our observations in general.

Recently, direct observations of flux ropes with the *SDO* data have been reported by many authors (Li & Zhang 2013a, 2013b, 2013c; Yang et al. 2014). However, the slipping motion of the footpoints of a flux rope is firstly observed in our work. We suggest that the slippage of the footpoints of the FR1 are triggered by the slipping magnetic reconnection during the flare process. For the footpoints of the FR1 are close to the footpoints of reconnected magnetic fields, the slipping magnetic reconnection successively heats the footpoints of the FR1 and the pre-existing invisible structures becomes visible. The successively visible structures form a surface of a "triangle flag" and indicates the FR1 has a "triangle-flag" topology. The fine structures of the FR1 rise upwards much faster than the whole flux rope does, and seem to be continuously fed from below while their easternmost footpoints keep slipping along the flare ribbon. This is a clear and a first ever-observational signature of the decoupling between the slowly moving plasma and the fast slipping loops.

We suggest that the "triangle-flag surface" may correspond to one-half of the coronal QSL, and the expanding FR1 is composed of field lines that are anchored in the regions surrounded by the hook of the QSL. According to the results of Titov (2007), the QSL is rooted at the horseshoe-like features and has a helical shape (Figures 4 and 5 in Titov 2007). The configuration of the QSL in Titov (2007) is similar to the "triangle-flag surface" in our observations. The QSL in Janvier et al. (2013, 2014) is along the J-hooked structures in the photosphere, which is also very similar to the configuration of the hooked flare ribbon in our work. The evolution of the fine structures of the FR1 is comparable to the model of Janvier et al. (2013). In their simulations, the field lines are successively formed via continuous series of reconnection and their footpoints in one polarity move inside the QSL footprint, following the hook shape of the QSL. The footpoints of field lines in the other polarity are fixed, which correspond to the west fixed footpoints in positive-polarity fields in our observations. The slipping velocities in Janvier et al. (2013) are different from our observations. In their model, the time-evolution of the slipping velocities shows a high peak value that is almost 390 times as large as the Alfvénic speed (Figures 7 and 8 in Janvier et al. 2013). The apparent motion of magnetic field lines is super-Alfvénic, and satisfies the slipping-running reconnection regime (Aulanier et al. 2006). However, the slipping motion in our observations satisfies the slipping reconnection regime (Aulanier et al. 2006). Our observations have provided a 3D magnetic reconnection signal, and more comprehensive understanding needs more observational examples and theoretical studies.

We acknowledge the *SDO*/AIA and HMI for providing data. This work is supported by the National Basic Research Program of China under grant 2011CB811403, the National Natural Science Foundations of China (11303050, 11025315, 11221063 and 11003026), the CAS Project KJCX2-EW-T07 and the Strategic Priority Research Program−The Emergence of Cosmological Structures of the Chinese Academy of Sciences, Grant No. XDB09000000.

REFERENCES

Asai, A., Yokoyama, T., Shimojo, M., et al. 2004, ApJ, 611, 557

Aulanier, G., Golub, L., DeLuca, E. E., et al. 2007, Science, 318, 1588

Aulanier, G., Pariat, E., Démoulin, P., & DeVore, C. R. 2006, Sol. Phys., 238, 347

Aulanier, G., Janvier, M., & Schmieder, B. 2012, A&A, 543, A110

Boerner, P., Edwards, C., Lemen, J., et al. 2012, Sol. Phys., 275, 41

Carmichael, H. 1964, NASA Special Publication, 50, 451

Cheng, X., Zhang, J., Liu, Y., & Ding, M. D. 2011, ApJ, 732, L25

De Moortel, I., & Galsgaard, K. 2006, A&A, 451, 1101

Démoulin, P., Bagala, L. G., Mandrini, C. H., Henoux, J. C., & Rovira, M. G. 1997, A&A, 325, 305

Démoulin, P., Henoux, J. C., Priest, E. R., & Mandrini, C. H. 1996, A&A, 308, 643

Dudík, J., Janvier, M., Aulanier, G., et al. 2014, ApJ, 784, 144

Gibson, S. E., Fan, Y., Mandrini, C., Fisher, G., & Demoulin, P. 2004, ApJ, 617, 600

Guo, Y., Ding, M. D., Cheng, X., Zhao, J., & Pariat, E. 2013, ApJ, 779, 157

Hirayama, T. 1974, Sol. Phys., 34, 323

Janvier, M., Aulanier, G., Bommier, V., et al. 2014, ApJ, 788, 60

Janvier, M., Aulanier, G., Pariat, E., & Démoulin, P. 2013, A&A, 555, A77

Lemen, J. R., Title, A. M., Akin, D. J., et al. 2012, Sol. Phys., 275, 17

Li, L. P., & Zhang, J. 2013a, A&A, 552, L11

Li, T., & Zhang, J. 2013b, ApJ, 770, L25

Li, T., & Zhang, J. 2013c, ApJ, 778, L29

Milligan, R. O., & Dennis, B. R. 2009, ApJ, 699, 968

Ning, Z., Cao, W., Huang, J., et al. 2009, ApJ, 699, 15

O'Dwyer, B., Del Zanna, G., Mason, H. E., Weber, M. A., & Tripathi, D. 2010, A&A, 521, A21

Parenti, S., Schmieder, B., Heinzel, P., & Golub, L. 2012, ApJ, 754, 66

Pesnell, W. D., Thompson, B. J., & Chamberlin, P. C. 2012, Sol. Phys., 275, 3

Pontin, D. I., Hornig, G., & Priest, E. R. 2005, Geophysical and Astrophysical Fluid Dynamics, 99, 77

Priest, E. R., & Démoulin, P. 1995, J. Geophys. Res., 100, 23443

Scherrer, P. H., Schou, J., Bush, R. I., et al. 2012, Sol. Phys., 275, 207

Schmieder, B., Heinzel, P., van Driel-Gesztelyi, L., & Lemen, J. R. 1996, Sol. Phys., 165, 303

Titov, V. S. 2007, ApJ, 660, 863

Yang, S., Zhang, J., Liu, Z., & Xiang, Y. 2014, ApJ, 784, L36

This preprint was prepared with the AAS LaTeX macros v5.2.

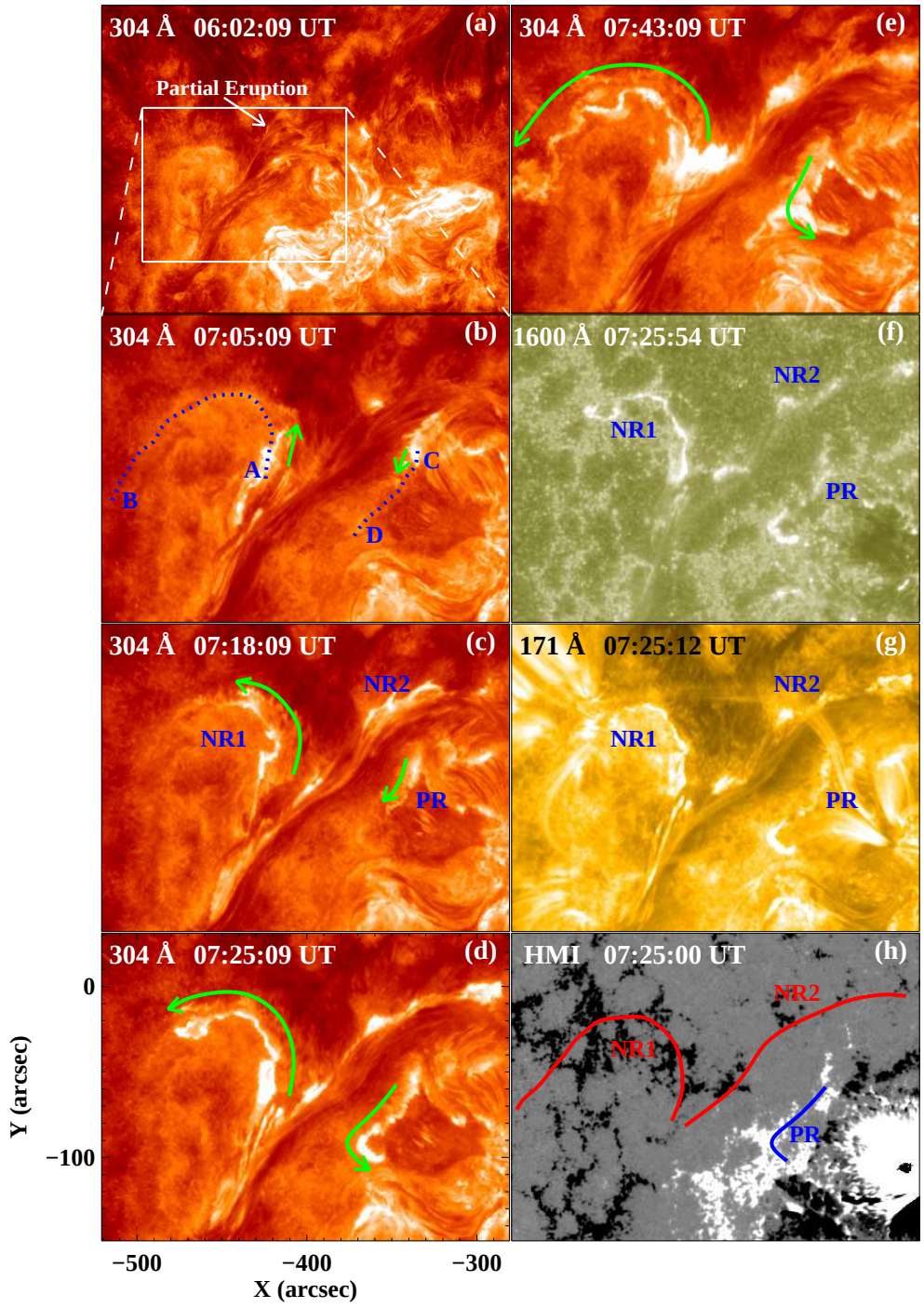

Fig. 1.— Evolution of flare ribbons (NR1, NR2 and PR) during the C8.9 flare on 2014 February 02 (see Animation 304). The white square in panel (a) denotes the FOV of the images in other panels. NR1 and NR2 are two negative-polarity ribbons and PR is one positive-polarity ribbon (panel (h)). Green arrows point to the opposite propagating directions of NR1 and PR. Blue dotted lines "A−B" and "C−D" in panel (b) show the positions of the cuts used to obtain the stack plots shown in Figure 4.

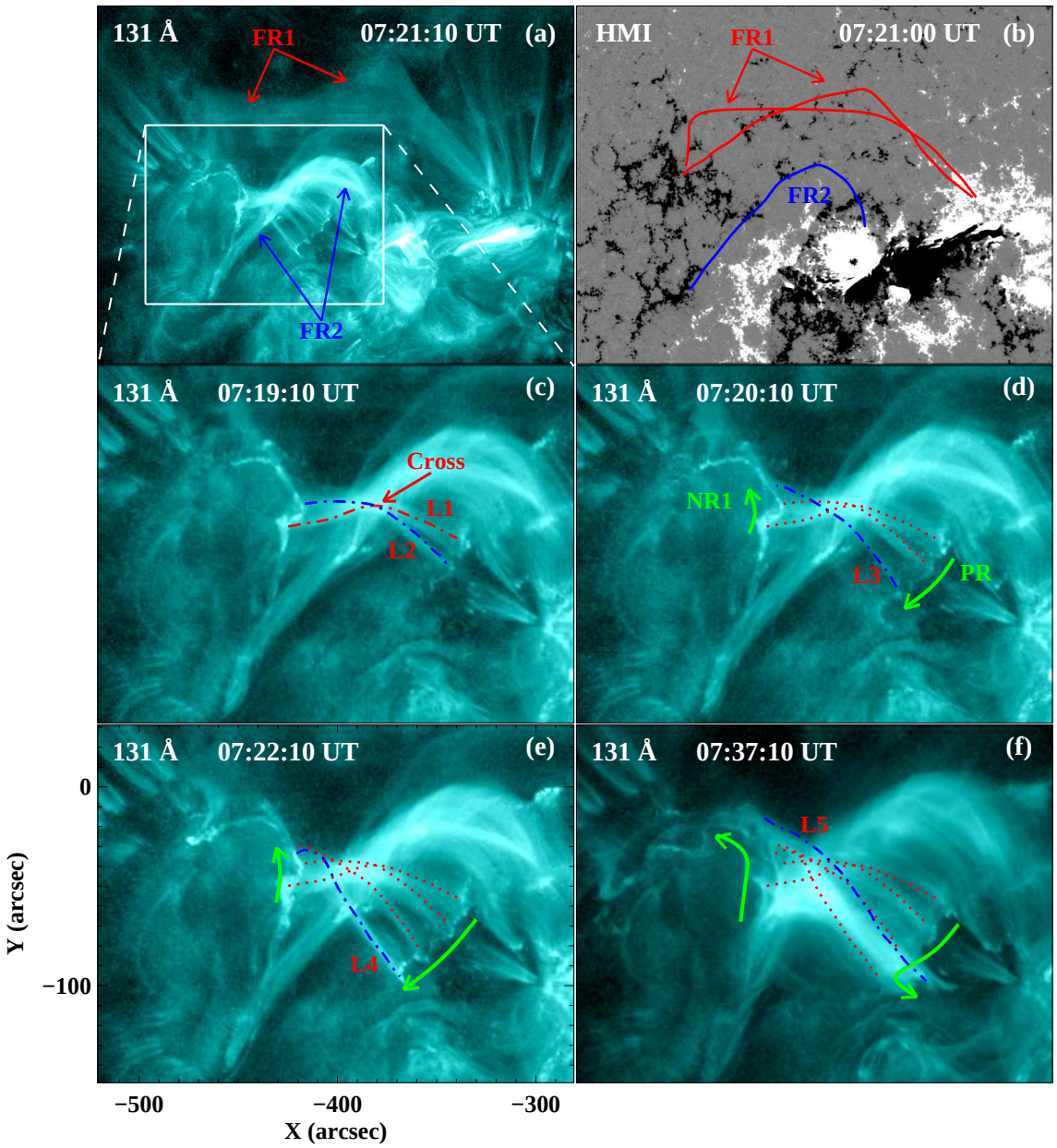

Fig. 2.— Overview of the slipping motion of flare loops (see Animation 131-loops). FR1 and FR2 are two flux ropes involved in this event. The red and blue solid lines in panel (b) respectively denote the main axes of the FR1 and FR2 at 07:21 UT. Dash-dotted lines in panels (c)-(f) outline the flare loops connecting the NR1 with PR and dotted lines are the duplicates of the flare loops at earlier times. Panel (f) shows the "bi-fan" shape of flare loops. Green arrows denote the opposite slipping directions of the loops.

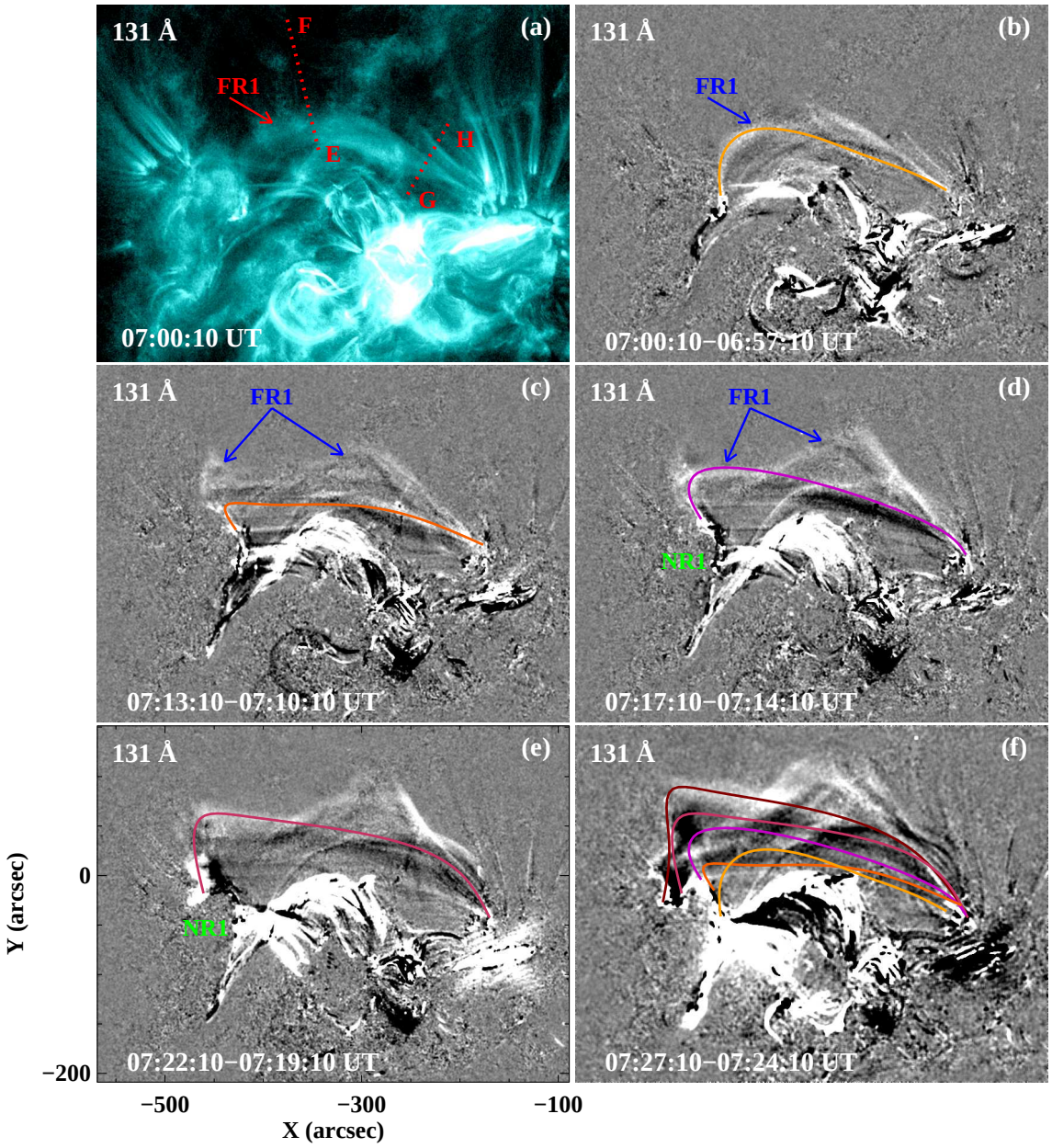

Fig. 3.— Slipping eruption of the FR1 in AIA 131 Å original and difference images (see Animation 131-fluxropes). Red dotted curve "E−F" and straight line "G−H" show the positions of the cuts used to obtain the stack plots shown in Figure 4. The solid curves in panels (b)-(f) denote the successive appearance of the fine structures of the FR1. Panel (f) shows the "triangle-flag surface" of the FR1.

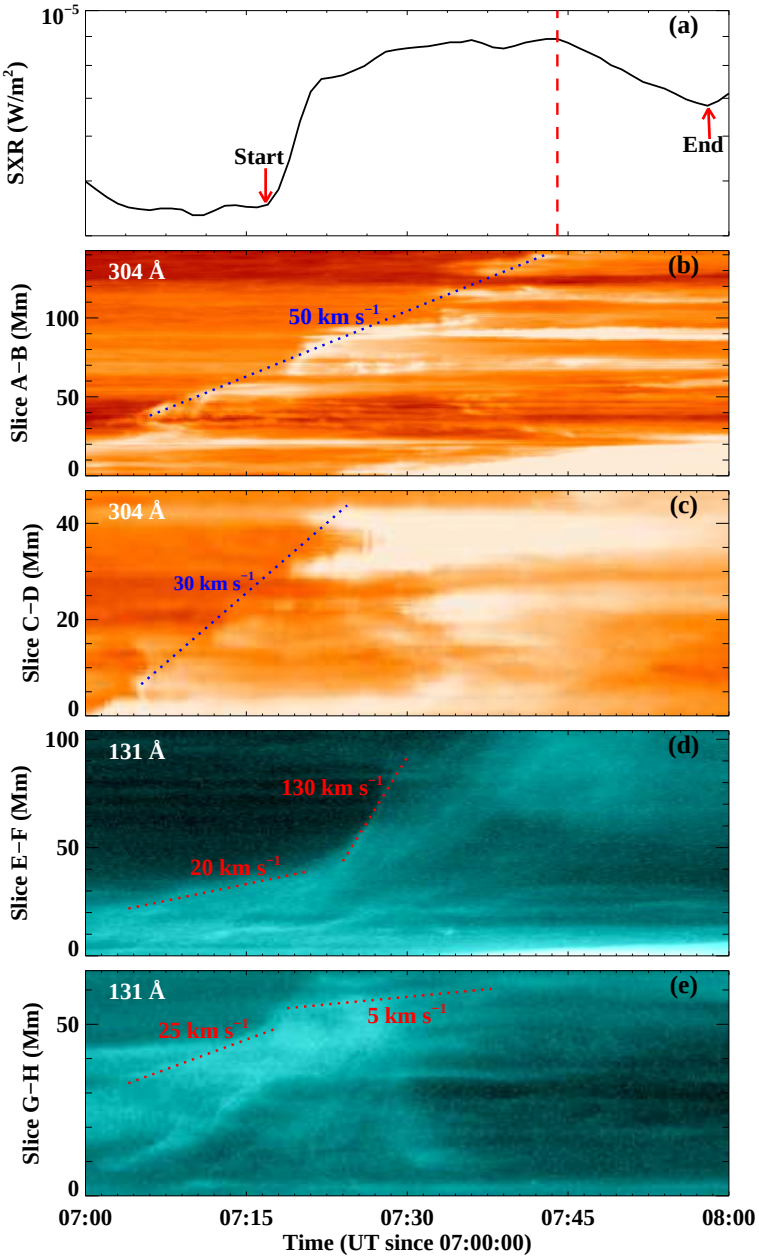

Fig. 4.— Panel (a): GOES SXR 1−8 Å flux of the associated flare. Red dashed line denotes the flare peak time. Panels (b)−(c): stack plots along slices "A−B" and "C−D" (blue dotted lines in Figure 1(b)) at 304 Å respectively showing the propagations of flare ribbons NR1 and PR. Panels (d)−(e): stack plots along slices "E−F" and "G−H" (red dotted lines in Figure 3(a)) at 131 Å respectively showing the rise of the fine structures and the whole FR1.